ChemPubSoc Europe

FULL PAPERS

So simple? Since the basic idea of ultra-high-vacuum (UHV) electrochemical modeling emerged, it has been claimed that UHV model experiments are too simple because they do not include the electrode potential. This combined scanning tunneling microscopy and density functional theory study gives insight into the influence of the electric field on single molecules in the diffusive layer. A field reorients adsorbed water molecules on water bilayers on Cu(111) at a distance of about 1 nm from the surface.

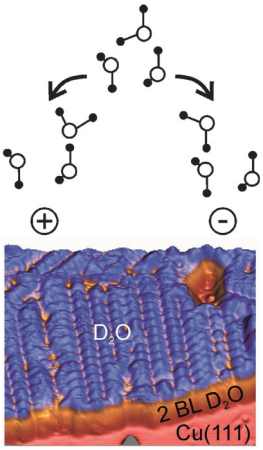

*M. Mehlhorn, S. Schnur, A. Groß, K. Morgenstern**

■■ – ■■

Molecular-Scale Imaging of Water Near Charged Surfaces

DOI: 10.1002/celc.201300063

Molecular-Scale Imaging of Water Near Charged Surfaces

Michael Mehlhorn,[c] Sebastian Schnur,[b] Axel Groß,[b] and Karina Morgenstern*[a]

The orientation of water molecules on water bilayers is investigated on Cu(111) by a combination of scanning tunneling microscopy and density functional theory. Theory predicts that the application of a field reorients the adsorbed water molecules at a distance of close to a nanometer from the surface. Experimental evidence is presented for this prediction. Furthermore, the process differs strongly between adsorption on two and on three ordered layers. We propose that these results give insight into the behavior of the diffusive layer close to electrodes.

1. Introduction

There is a broad and long-lasting interest in supported water–ice in areas as diverse as environmental sciences,[1] astrochemistry,[2] and electrocatalysis. In electrocatalysis, the electrodes control conversion between chemical and electrical energy, and an atomistic understanding is emerging.[3] Conventionally, the so-called Helmholtz or Stern double layer is mainly discussed in view of the capacitance caused by the unequal distribution of ions.[4] This double layer was intensely investigated[5] and novel experimental techniques, in particular X-ray, neutron scattering, and infrared spectroscopy, increased the knowledge about it.[6,7] However, the influence of the hydration onto the reaction at the electrodes has been ignored for a long time. It is still a mystery how water molecules contribute to the electric double layer, although water molecules dominate on electrode surfaces under any potential condition.[7] It is only emerging that the hydration shell of the ions and of the electrode itself might be active elements.[8] In particular, the orientation of the water molecules and thus the orientation of their dipole will influence the total capacitance.[9] The development of a full understanding of the active chemical role played by water in electrocatalysis is thus important for a full understanding of the processes happening at electrodes.

As a first step, it is essential to understand how water molecules are arranged at charged interfaces and how this arrangement changes with electrode potential. Thereby, not only the first highly ordered layers are of interest but also the diffuse (near-electrode) layers that are nearly unexplored on the atomistic level. This diffusive layer influences at least the diffusion of the solvated ions towards the electrodes.[10] However, it is virtually impossible to gain microscopic information of the water structure in the fluid phase.

On the other hand, scanning tunneling microscopy (STM) has given tremendous information about the structure of condensed water, in particular on the (111) faces of Pt, Ag, Pd, Cu, and Au.[7,11–15] Depending on the adsorption or annealing temperature, amorphous or crystalline structures grow on such surfaces.[16] While the amorphous ice structures were often used in laboratory experiments to mimic fluid water,[16] we argue here that the crystalline structures are good model systems for the ordered layers at electrode surfaces. We base this on the fact that it is well established that water forms a tetrahedral network also in liquid phases.[17] Molecules above these layers are consequently representative for the diffuse layer above electrode surfaces.

2. Results and Discussion

To set the stage, we first determine the optimal orientation of the hydrogen atoms within the first ordered layer on a metallic surface, here Cu(111). The optimized combination of two bilayers is a series of H-up–H-down, in which all molecules are fourfold coordinated (Figure 1a). The optimized combination of three bilayers is less certain. The combination of H-up–H-up–

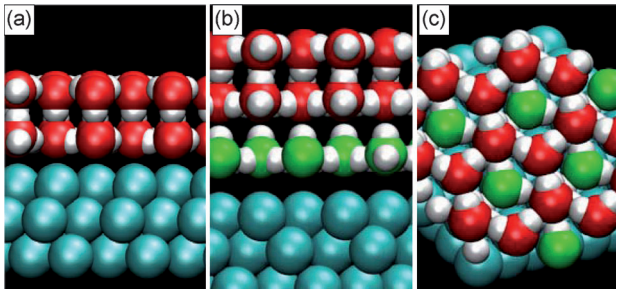

Figure 1. Optimized structure for: a) two bilayers, b,c) three bilayers. Cu atoms in blue, oxygen on water molecules in red (two upper layers) and green (third layer from top).

[a] *Prof. Dr. K. Morgenstern*
Lehrstuhl für physikalische Chemie I
Ruhr-Universität Bochum
44780 Bochum (Germany)
Fax: (+49) 234-32-14182
E-mail: karina.morgenstern@rub.de

[b] *Dr. S. Schnur, Prof. Dr. A. Groß*
Institut für theoretische Chemie
Universität Ulm, Albert-Einstein-Allee 11
89069 Ulm (Germany)

[c] *Dr. M. Mehlhorn*
Institut für Experimentalphysik
FU Berlin, Arminallee 14
14195 Berlin (Germany)

H-down shown in Figures 1b and Figure 1c is only ~5 meV more stable than a combination of H-up–H-down–H-down. Note that the lowest bilayer (green) is thereby shifted by one lattice spacing with respect to the double bilayer. The influence of the middle layer on the single adsorbed molecules is, however, of minor importance here.

Next, we optimize the binding geometry of water molecules adsorbed on the double and triple bilayer without external field. Though only a single molecule is adsorbed per unit cell, this mimics rows of molecules due to the periodic boundary conditions. The most stable adsorption geometry consists of a molecule that binds with its oxygen atom to a water molecule in the second bilayer and with one of its hydrogen atoms to the neighboring bilayer molecule. Upon adsorption of this water molecule, the main binding molecule in the upper bilayers turns around from H-down to H-up (Figure 2a).

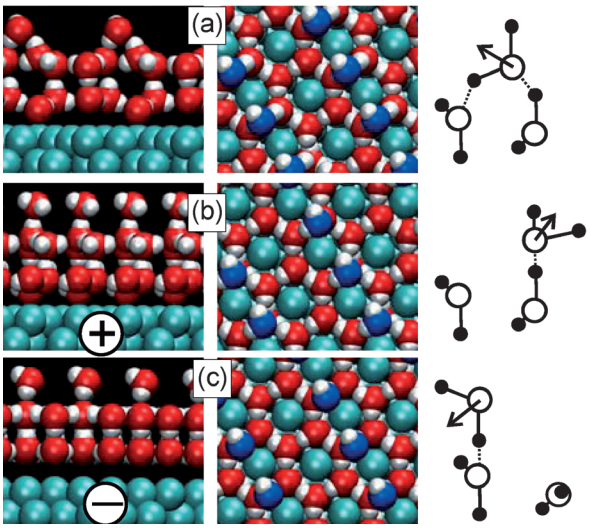

Figure 2. Different binding possibilities of molecules on the second bilayer a) without external potential; b) with positive external potential; c) with negative external potential. The schema on the right-hand side illustrates hydrogen bonding as dashed lines; the arrows depict the orientation of the dipole.

Finally, an influence of the external field onto the binding geometry is simulated by either adding or removing charge from/to the metal. As there is no direct information about the correspondence of the STM bias voltage to the charge, the trends discussed below are of qualitative nature.

We simulate application of a positive potential by removing electrons from the metal–water system. Interestingly, the adsorbed molecule does no longer hydrogen-bond to the bilayer, only the hydrogen bond provided by the water molecule remains. The adsorbed water molecule is now oriented in parallel to the surface (Figure 2b). This leads to a lateral shift of its center-of-mass by 90 pm. Furthermore, the adsorbed molecule in this structure is 60 pm more distant from the surface.

We simulate application of a negative field or potential by adding electrons to the system. Here, the most stable structure consists of a molecule that binds with one hydrogen atom to the bilayer beneath to better align with the electric field (Figure 2c). Thereby, the molecules in the surface remain in their H-down position. In both fields, the additional water molecules thus lose one hydrogen bond by the field, but a different one (Figures 2c and 2b).

For a systematic investigation, we compare these three cases for the water molecules adsorbed on the second and third bilayers (see Table 1). On both layers, geometry (a) is most stable. On the second and third layer, a change to structure (b) is realized at −0.2 e- and −0.55 e-, respectively. This larger potential needed (despite of a different potential drop for layers of different width) indicates that the barrier for the structural change is larger on the third than on the second layer. Nonetheless, structure (b) has the same stability (within the theoretical precision) on both layers. In contrast, the energy difference between (a) and (c) is much larger on the third layer than on the second one. On the second layer, structure (c) is more stable starting with a charge of +0.15 e^-. On the third layer, the turning point is not reached within charges up to +1 e^-. Thus, for both polarities, the influence of the additional charge/electrode potential is more important for the molecules on the second than on the third bilayer. This is attributed to the fact that the surface charge is better screened by three water layers than by two layers.

Table 1. Parameters for the binding geometries of the water molecules shown in Figure 2 on different layers under different fields: Energy differences and lateral displacements are presented with respect to structure (a) and per adsorbed water molecule. The charge is given per unit cell, which contains 18 Cu atoms. The height difference is based on the distance of the oxygen atoms.

Binding type	(a)	(b)	(c)	(a)	(b)	(c)
on nth layer		2nd			3rd	
energy difference [meV]	0	140	111	0	137	254
stable at V	0	+	-	0	+++	—
transition at charge [e^-]	0	-0.2	+0.15	0	-0.55	> +1e^-
lateral displacement [pm]	0	90	10	0	110	–
distance to uppermost Cu layer [nm]						
uppermost O atom	0.98	0.93	0.92	1.21	1.25	–
uppermost H atom	1.02	0.98	0.97	1.23	1.24	–
real height difference:						
from [pm]	220	280	280	230	270	290
to [pm]	290	350	300	330	340	350

The largest geometrical change is expected for structure (b) on the second layer. For all other combinations, the change in upper values is negligible. The small change in lower value will not be detectable in STM experiments. The vertical displacement is in line with a calculated center-of-mass arrangement of the wetting water layer above charged Pd(111).[18] Finally, only structure (b) shows a measurable lateral displacement with respect to structure (a).

Although theory might predict different geometries at different charges, only experiment is able to prove that these changes are present under realistic conditions. As STM is not able to image hydrogen atoms within molecules, we utilize the fact that the appearance of the molecules depends on the ori-

entation of their orbitals with respect to tunneling current direction.[19] For example, contrast inversion of metal-supported water clusters on Ag(111) was shown to result from different tilting angles of the molecules.[12,13]

We present evidence for the water reorientations on top of a double or a triple bilayer for the nominal coverage of one bilayer of water on Cu(111). This layer does not wet the surface, but forms islands that are up to four bilayers in height.[14] It reconstructs at 130 K into islands with a structure sketched in Figure 3a. The structure consists of two and three bilayers both decorated by rows of twofold periodicity.[14] While molecules have different numbers of hydrogen-bonded neighbors in the same layer, as indicated in the model, we here concentrate on the molecules with no direct neighbors, that is, neighbors that are close enough to form in-plane hydrogen bonds. These molecules form rows of twofold periodicity with respect to the bilayer mimicking the situation explored theoretically. These rows of molecules are indeed imaged differently by STM at opposite polarity, as shown in Figures 3b and 3c. Instead of lines of protruding dots at +1 V (Figure 3b), distinct rows of black dots are imaged at −1 V (Figure 3c). The change in contrast is reversible. Clearly, the field reorients the water molecules transiently. Figure 3 thus confirms that the singly bonded molecules can be turned in the field.

More gradual changes to the apparent height are observed by changing the voltage in the range of a few hundred millivolt. A series featuring 18 images between −1.5 and +1.3 V reveals that there are two changes at threshold voltage of −0.1 and +0.5 V, respectively.[20] The asymmetric threshold voltage is in qualitative agreement with different thresholds for reorientation predicted by theory. This agreement corroborates that we observe in experiment the predicted reorientation.

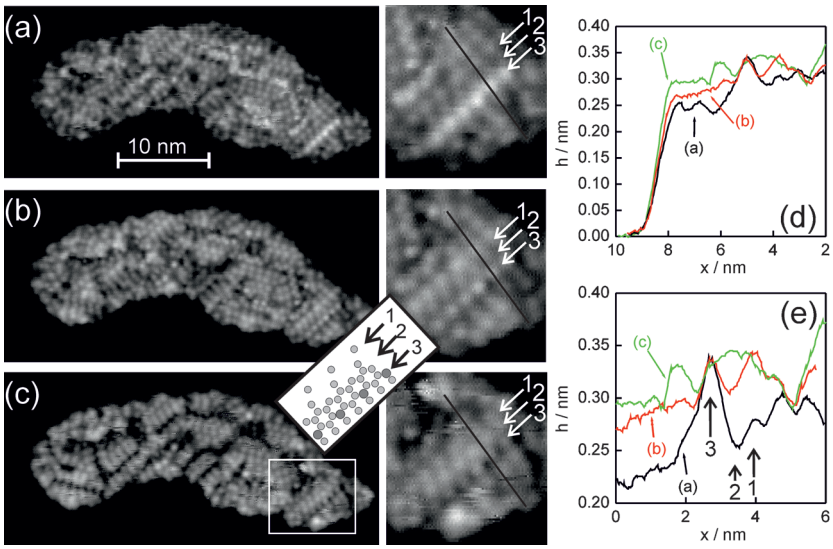

Figure 4. Voltage-dependent imaging of an ice island with enlargement as indicated in (c). Inset: schematic top view of a layer with the same row numbering as in images (with $I = 2.8$ pA): a) −432 mV, b) 166 mV, and c) 744 mV. d,e) Line scans as indicated in the magnifications.

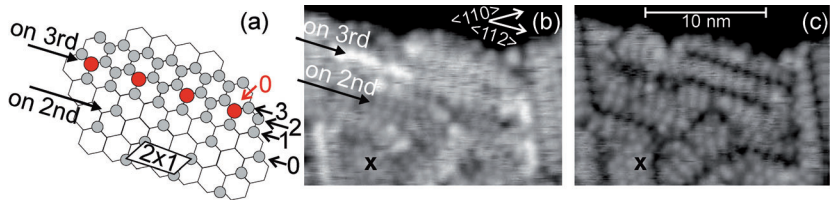

Figure 3. Crystalline ice on Cu(111): a) Structural model with singly bond molecules on top and in (2×1) superstructure as indicated by the arrows on the second (gray balls) and third bilayer (red balls), respectively. The hexagonal grid indicates two complete bilayers; gray (red) balls represent molecules in the third (fourth) bilayer; numbers on the right-hand side indicate the number of in-plane binding partners; the ridges follow the three <112> directions of the copper support. b,c) Rim of an ice island at opposite polarity with the same defect marked by a cross; $I = 2$ pA, $V = 1$ V (b) and $V = -1$ V (c).

To analyze the resulting structures, we show a complete island in molecular resolution in Figures 4a–c for a voltage below, within, and above the thresholds, respectively. We note that molecules within each of the rows marked 1 to 3 show equivalent behavior (see magnifications). Below both thresholds (Figure 4a) row '3' is clearly most protruding. Between the thresholds (Figure 4b) rows '1' and '3' have approximately the same apparent height. Above both thresholds (Figure 4c), the row marked '2' appears in between them. These rows assigned to the molecules in row '1' are on top of the second bilayer and in row '3' on top of the third bilayer (c.f. Figures 3a and 4, inset[14]). Thus, singly hydrogen-bonded molecules in different layers corresponding here to row '1' and row '3' show a different dependence on voltage. Line scans (Figure 4e) across the rows are normalized to the surface value (Figure 4d). With respect to this value, row '1', a row that is situated on top of the double layer, increases in apparent height by 0.6 nm from −423 to 166 mV. Row '3', a row that is situated on the third layer does not change in apparent height at all. This is in perfect qualitative agreement with the changes in geometric height predicted theoretically.

Finally, evidence of a lateral shift is presented in Figure 5. As best seen in the line scan (Figure 5c), the apparent trough not only deepens with increasing voltage, but also shifts laterally in agreement with the calculated lateral shift in atomic position (see Table 1).

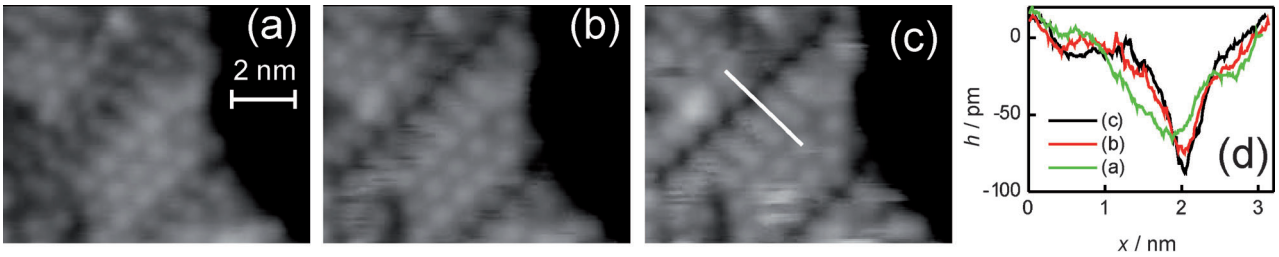

Figure 5. Voltage-dependent imaging at positive polarity (with $I = 0.24$ nA): a) 167 mV, b) 240 mV, and c) 871 mV. d) The line scans where indicated in (c).

3. Conclusions

In conclusion, we theoretically predict and experimentally observe a different behavior of water molecules adsorbed on a second and on a third ordered layer on a metal surface with respect to the applied potential. Such information was experimentally not available yet and enables unprecedented insight into the behavior of solvent molecules in the diffusive layer above an electrode and on the influence of the electrode potential onto them. The change in orientation in the upper bilayer implies that the diffusive layer leads to regular changes in the ordered layers on electrodes at positive polarity, because theory shows that the rotation of the molecules is accompanied by a structural change of the crystalline layers. Our results are the first microscopic evidence for subtle changes in water-molecule orientations in the diffusive layer.

On a more general footing, our results suggest that high-resolution, low-temperature scanning tunneling microscopy, in combination with density functional calculations, is viable to provide microscopic information about the solvent properties in the electrolyte close to electrode regions. In the future, the method should be used for solutes within water.

Experimental Section

The experiments were performed with a custom-built low-temperature STM,[21] which facilitates imaging at 0.2 pA. This stability is important here because of the large difference in apparent-to-real height of almost 1 nm for the insulating water structures.[14] The STM was housed in a UHV chamber with a base pressure of 10^{-10} mbar and standard facilities for sample cleaning. The single-crystalline Cu(111) surface was cleaned by cycles of Ne^+ sputtering and annealing. D_2O was degassed in vacuum through freeze–thaw cycles. A nominal coverage of one bilayer was deposited onto the sample held at 88 K. Finally, the sample was annealed to 130 K for 15 min to produce well-characterized ice structures[14] and transferred into the STM, where measurements were performed at 5 K. The intrinsic field in the tip–sample region was utilized to mimic different electrode potentials.[22] Voltages were applied to the sample with respect to the tip. Thus, a negative voltage pulls the electronic charge into the sample. Periodic DFT calculations were performed using the Vienna ab initio simulation package (VASP) code,[23] employing the generalized gradient approximation (GGA) to describe the exchange-correlation effects by employing the exchange-correlation functional by Perdew, Burke and Ernzerhof (PBE).[24] The ionic cores are represented by projector augmented wave (PAW) potentials[25] as constructed by Kresse and Joubert.[26] The electronic one-particle wave functions are expanded in a plane–wave basis setup to an energy cutoff of 400 eV. The Cu(111) substrate is represented by a three-layer slab, a $\sqrt{3}$ x $\sqrt{3}$ surface unit cell is used for determination of the stacking order, and a $2\sqrt{3}$ x $\sqrt{3}$ unit cell for determination of the molecule's adsorption sites.

Acknowledgements

This research has been supported by the Konrad–Adenauer–Stiftung and through the Research Unit 1376, contract GR 1503/21–1, contract MO 960/18–1 and by the Cluster of Excellence RESOLV (EXC 1089) funded by the Deutsche Forschungsgemeinschaft. Computer time on the BW-Grid of the federal state of Baden-Württemberg is gratefully acknowledged.

Keywords: adsorption · density functional calculations · scanning probe microscopy · single-molecule studies · water

[1] B. J. Murray, D. A. Knopf, K. Bertram, *Nature* **2005**, *434*, 202–205.
[2] a) E. Mayer, R. Pletzer, *Nature* **1986**, *319*, 298–301; b) R. Papoular, *Mon. Not. R. Astron. Soc.* **2005**, *362*, 489–497.
[3] D. M. Kolb, *Surf. Sci.* **2002**, *500*, 722–740.
[4] H. Ni, R. C. Amme, *J. Colloid Interface Sci.* **2003**, *260*, 344.
[5] M. F. Toney, J. N. Howard, J. Richer, G. L. Borges, J. G. Gordon, O. R. Melroy, D. G. Wiesler, D. Yee, L. B. Sorensen, *Nature* **1994**, *368*, 444–446.
[6] M. Ito, M. Yamazaki, *Phys. Chem. Chem. Phys.* **2006**, *8*, 3623.
[7] M. Ito, *Surf. Sci. Rep.* **2008**, *63*, 329–389.
[8] B. W. Ninham, T. T. Duignan, D. F. Parsons, *Curr. Opin. Colloid Interface Sci.* **2011**, *16*, 612–617.
[9] a) S. Schnur, A. Groß, *New J. Phys.* **2009**, *11*, 125003–1–25; b) S. Schnur, A. Groß, *Catal. Today* **2011**, *165*, 129–137; c) A. Roudgar, A. Groß, *Chem. Phys. Lett.* **2005**, *409*, 157–262.
[10] M. van Soestbergen, P. M. Biesheuvel, M. Z. Bazant, *Phys. Rev. E* **2010**, *81*, 021503–1–13.
[11] a) M. Morgenstern, Th. Michely, G. Comsa, *Phys. Rev. Lett.* **1996**, *77*, 703–706; b) K. Morgenstern, K. H. Rieder, *J. Chem. Phys.* **2002**, *116*, 5746–5752; c) K. Morgenstern, *Surf. Sci.* **2002**, *504*, 293–300; d) K. Morgenstern, K. H. Rieder, *Chem. Phys. Lett.* **2002**, *358*, 250–256; e) T. Mitsui, M. K. Rose, E. Fomin, D. F. Ogletree, M. Salmeron, *Science* **2002**, *297*, 1850–1852; f) J. Stähler, M. Mehlhorn, U. Bovensiepen, M. Meyer, D. O. Kusmierek, K. Morgenstern, M. Wolf, *Phys. Rev. Lett.* **2007**, *98*, 206105–1–4; g) A. Michaelides, K. Morgenstern, *Nat. Mater.* **2007**, 6, 597–601; h) H. Gawronski, J. Carrasco, A. Michaelides, K. Morgenstern, *Phys. Rev. Lett.* **2008**, *101*, 136102–1–4; i) M. Mehlhorn, H. Gawronski, K. Morgenstern, *Phys. Rev. Lett.* **2008**, *101*, 196101–1–4.
[12] K. Morgenstern, J. Nieminen, *Phys. Rev. Lett.* **2002**, *88*, 066102–1–4.
[13] K. Morgenstern, J. Nieminen, *J. Chem. Phys.* **2004**, *120*, 10786–10791.
[14] M. Mehlhorn, K. Morgenstern, *Phys. Rev. Lett.* **2007**, *99*, 246101-1-4.
[15] a) A. Hodgson, S. Haq, *Surf. Sci. Rep.* **2009**, *64*, 381–451; b) M. Tatarkhanov, D. F. Ogletree, F. Rose, T. Mitsui, E. Fomin, S. Maier, M. Rose, J. I. Cerda, M. Salmeron, *J. Am. Chem. Soc.* **2009**, *131*, 18425–18434; c) S. Standop, A. Redinger, M. Morgenstern, T. Michely, C. Busse, *Phys. Rev. B*

2012, *82*, 161412(R)-1 – 4; d) H. Okuyama, I. Hamada, *J. Phys. D* **2011**, *44*, 464004 – 1 – 14; e) S. Maier, I. Stass, T. Mitsui, P. J. Feibelman, K. Thürmer, M. Salmeron, *Phys. Rev. B* **2012**, *85*, 155434 – 1 – 5.
[16] M. A. Henderson, *Surf. Sci. Rep.* **2002**, *46*, 1 – 308.
[17] D. Eisenberg, W. Kauzmann, *The structure and Properties of Water*, Oxford University Press, New York, **1969**.
[18] a) J. S. Filhol, M.-L. Bocquet, *Chem. Phys. Lett.* **2007**, *438*, 203 – 207; b) M.-L. Bocquet, N. Lorente, *J. Chem. Phys.* **2009**, *130*, 124702 – 1 – 6.
[19] J. A. Nieminen, E. Niemi, K.-H. Rieder, *Surf. Sci.* **2004**, 552, L47 – L52.
[20] A series of STM images transformed into a movie can be found in the supporting online material 'Contrast inver-V.avi'.
[21] M. Mehlhorn, H. Gawronski, L. Nedelmann, A. Grujic, K. Morgenstern, *Rev. Sci. Instrum.* **2007**, *78*, 033905 – 1 – 7.
[22] The external electric field is proportional to the enclosed charge density ($E = 4\pi\sigma/\varepsilon_0\backslash\varepsilon_k$).Absolute values cannot be given, because the field depends on the exact shape of the tip.However, we estimate the field at the surface below the tip to be around 1 V nm^{-1} at the tunnelling conditions employed here, c. f. [14].
[23] G. Kresse, J. Furthmüller, *Phys. Rev. B* **1996**, *54*, 11169 – 11186.
[24] J. P. Perdew, K. Burke, M. Ernzerhof, *Phys. Rev. Lett.* **1996**, *77*, 3865 – 3868.
[25] P. E. Blöchl, *Phys. Rev. B* **1994**, *50*, 17953 – 17979.
[26] G. Kresse, D. Joubert, *Phys. Rev. B* **1999**, *59*, 1758 – 1775.

Received: May 29, 2013
Published online on ■■ ■■, 0000